

## Spectral Characteristics of 50 GHz FSR Etalon for Wide-band DWDM Application

Jong Deog Kim\* and Jong Tae Moon

*Integrated Optical Module Team, Basic Research Laboratory,  
Electronics and Telecommunications Research Institute, Daejeon, 305-350, KOREA*

(Received May 7, 2004)

The periodic transmission spectrum of a solid etalon for wide-band capability is analyzed both theoretically and experimentally. In the transmission spectrum with an incident area of a photodetector, the peak wavelength and transmittance are deeply dependent on the incident angle and the divergence angle of the input laser beam. A thermal adjustment for a solid etalon is an optional way to control the transmission spectrum instead of the inefficient fine-angle alignment. In the result, we present the deviations of free spectral range (FSR) by the change in angle and temperature over wide wavelength range.

OCIS codes : 070.4790, 060.4510, 120.2230, 260.3060

### I. INTRODUCTION

In the dense wavelength division multiplexing (DWDM) system, the channel spacing becomes narrower for a higher capacity of transmission, and widely tunable semiconductor lasers [1,2] are emerging as the attractive light sources for the next generation of optical networks. With the recent trends, the wavelength stabilization is very important to maintain the channel spacing without crosstalk between channels and to fix the wavelengths to ITU-grid during the long-term aging. For the compact and simple application in the DWDM system, a wavelength locker has been integrated in a wide tunable laser module [1], or a single mode laser module [3,4], and a solid etalon is used to monitor the wavelength channels with a free spectral range (FSR), such as 100 GHz, 50 GHz, or 25 GHz. The etalon-based technology for the wavelength monitor and control is the most attractive one among various methods as explained in [4], and it is also used for various DWDM applications, such as channel monitor, dispersion compensator, and wavelength interleaver, as well as wavelength locker. However, in spite of its broad applications, the practical spectral behaviors of the solid etalon for the multi-channel capability have not been well reported yet.

In this letter, we present the theoretical and experimental analyses about the spectral characteristics of the solid etalon to investigate the optimized assembly conditions for wide-band DWDM application, especially as a function of arbitrary incident angle for a diverged

laser beam into a 250  $\mu\text{m}$  incident area of photodetector (PD) for practical analysis.

### II. THEORETICAL ANALYSIS

Fig. 1 shows a simple schematic view for our analysis including an angle-tilted etalon and an incident area of PD in the optical path of a diverged Gaussian laser beam, on a thermo-electric cooler (TEC) for the temperature control, as in the practical applications for the optical component.

The optical intensity of Gaussian beam with the waist diameter  $2W_0$  is obtained from the complex amplitude to satisfy the Helmholtz equation, as a function of the axial distance and the radial distance  $\rho = (x^2 + y^2)^{1/2}$ , as well summarized in [5]. With the beam width  $W(z)$  and the wavefront curvature radius  $R(z)$  for a circular Gaussian beam, if we define  $\theta = \rho/R(z)$

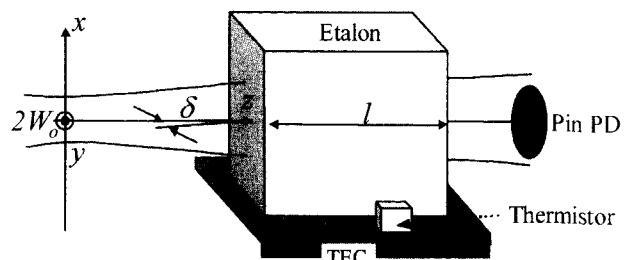


FIG. 1. A solid etalon and a photodetector in an incident Gaussian beam.

and  $\theta_o = W(z)/R(z)$ , the optical intensity is given as a function of the divergence angle and the axial distance  $z$ ,

$$I(z, \theta) = I_o(z) \exp\left[-\frac{2\theta^2}{\theta_o^2}\right] \equiv I_o(z) I_{\theta_o}(\theta) \quad (1)$$

where  $I_o(z)$  is the intensity on axis  $z$ . About 86% of the Gaussian beam power is confined within a cone with the angle  $\theta_o$  of beam width, which is converged to the constant divergence angle  $\theta_o = \lambda / \pi W_o$  at far from the Rayleigh range  $z_o$ ,  $z \gg z_o$ .

The spherical wave in Gaussian beam is locally like a plane wave with wavefront normal that is a paraxial ray. Thus, we can consider the separate transmittance of etalon for each wavefront normal as a spectral response of etalon for the perfect plane wave,

$$T_1(\lambda, \theta_i) = \left[1 + \left(\frac{2F}{\pi}\right)^2 \sin^2\left(\frac{\pi v}{v_F}\right)\right]^{-1} \quad (2)$$

where  $v = c/\lambda$ ,  $v_F = c/2n(\lambda)l \cos(\theta_r)$ , and  $F$  is finesse which characterizes the resonance bandwidth with the free spectral range (FSR.)  $v_F$ . The refractive index  $n(\lambda)$  of the fused silica etalon is taken from the dispersion equation by J.H.Wray and J.T.Neu [6], and the incident angle  $\theta_i$  of the each plane wave for the normal axis of the etalon has a relation of Snell's law with the refracted angle into the etalon of  $\theta_r$  [7]. For an arbitrary tilted angle  $\delta$  of the normal axis of the etalon about the Gaussian beam axis, we can easily consider the effect of the incident angle by the coordinate transformation with  $R(z)$ ,  $\theta$ ,  $\varphi$ , parameters in a spherical coordinate, so that (2) can be written in the form of  $T_{1\delta}(\lambda, \theta, \varphi)$  as a function of  $\delta$ .

The total transmitted beam intensity of a solid etalon for a Gaussian beam is the superposition of locally transmitted waves with each angular vector. Since, for the practical application in a laser module, we are interested in detection of the intensity by an incident area of the PD rather than for the whole Gaussian beam, the total transmittance for full angle  $2\theta_P$  corresponding to the PD located on the Gaussian beam axis is given by

$$T_{\theta}(\lambda, \delta) = \frac{\int_0^{\theta_P} \int_0^{2\pi} I_{\theta_o}(\theta) T_{1\delta}(\lambda, \theta, \varphi) \theta d\varphi d\theta}{\int_0^{\theta_P} \int_0^{2\pi} I_{\theta_o}(\theta) \theta d\varphi d\theta} \quad (3)$$

which  $\rho d\varphi d\theta = R(z) \theta d\varphi d\theta$  and all common factors for are erased from denominator and numerator.

The shift of the resonance peak following the incident angle of the laser beam is one of the interested parameters for the alignment of spectrum to a specific target wavelength like ITU channel in DWDM application. For a non-diverged beam,  $2\theta_o = 0^\circ$ , the wave-

length shift of the resonance peak for normal incident beam is introduced from (2) as a function of the incident angle and refractive index,

$$\Delta\lambda_p = -(\lambda_p/2)(\delta^2/n^2) \quad (4)$$

However, the resonance peak shift for a diverged beam doesn't follow the formula (4), and it is smaller with larger divergence angle by the superposition of the diffraction effect at the PD side, as presented in the next section.

### III. RESULTS AND DISCUSSION

In our analysis, the solid etalon consists of a fused silica glass with 2076  $\mu\text{m}$  of cavity length, and the front and rear facets have been coated with multi-thin film layers for reflectance of 0.4. The refractive index of the fused silica is  $n=1.4440$  at  $25^\circ\text{C}$  and 1550 nm of wavelength, and the temperature coefficient of the refractive index is  $11.5 \times 10^{-6}/^\circ\text{C}$  [6]. For simulation and measurement, a photodetector (PD) with an active area of 250  $\mu\text{m}$  is located on the optical axis at 0.5 mm distance after the etalon, and the laser source is located on the optical axis of 1.0 mm distance in the front of the etalon.

Fig. 2 shows the calculated transmission spectrum for a slightly diverged angle,  $2\theta_o = 0.5^\circ$ , and a largely diverged angle,  $2\theta_o = 13^\circ$ , of a Gaussian beam for the etalon at  $25^\circ\text{C}$ . In the case of  $2\theta_o = 0.5^\circ$ , the peak transmittance rapidly decreases with the increasing incident angle  $\delta$  of the Gaussian beam for the normal axis of the etalon, and the transmittance ratio between peak and bottom levels is already less than 1 dB at

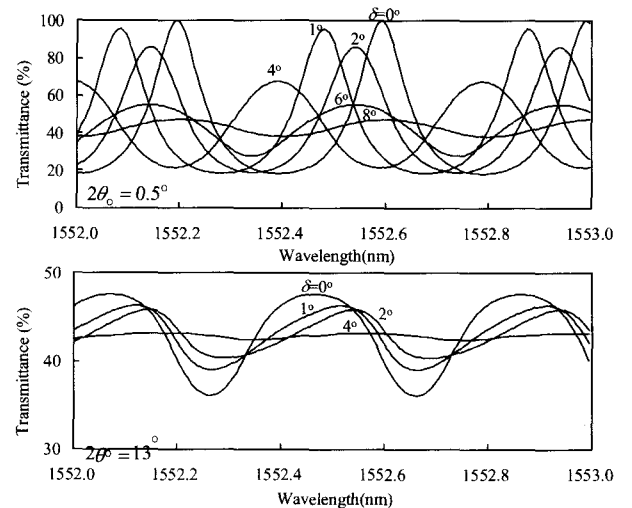


FIG. 2. Simulated transmission spectra of a solid etalon for several incident angles of a diverged Gaussian beam with  $2\theta_o = 0.5^\circ$  and  $2\theta_o = 13^\circ$ .

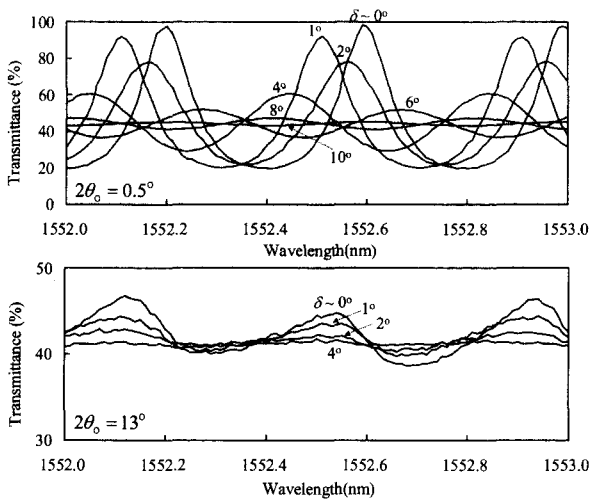


FIG. 3. Measured transmission spectra of a solid etalon for several incident angles of a diverged Gaussian beam with  $2\theta_0 = 0.5^\circ$  and  $2\theta_0 = 13^\circ$ .

$\delta = 8^\circ$ . The FSR and the bandwidth of the etalon increases with the incident angle, and the resonance peak wavelength  $\lambda_p$  is quickly shifted to shorter wavelength for  $\delta > 1^\circ$ .

For a greatly diverged angle,  $2\theta_0 = 13^\circ$ , the transmittance ratio for a wavelength change is very poor, so that it is already almost flat at  $\delta = 4^\circ$ . The peak wavelength shift for the incident angle is much smaller than for the slightly diverged beam, so there is even a positive shift for  $\delta < 8^\circ$  in the wavelength domain.

Fig. 3 shows the measured transmission spectrum of the solid etalon for the both diverged laser beams, evaluated as having  $2\theta_0 = 0.5^\circ$  with a fiber pigtailed collimator and  $2\theta_0 = 13^\circ$  with an as-cleaved single mode fiber (SMF). A tunable laser source having the wide wavelength range from 1492 nm to 1640 nm is used. All trends of the measured resonance curves is agree very well with the calculated results shown in Fig. 2, although there are some different wavelength positions of the resonance peaks in the case of  $2\theta_0 = 0.5^\circ$  and the slightly noisy transmittances in the case of  $2\theta_0 = 13^\circ$ , because of the extreme angle sensitivity at larger incident angle and the back reflection effect into the laser source from the etalon surface at greatly diverged laser beam.

For a diverged laser beam, the divergence angle of the incident laser beam is also a factor to induce the change of FSR with the incident angle. Fig. 4 shows the deviation of FSR as a function of the increased incident angle for each divergence angle,  $2\theta_0 = 0^\circ, 2^\circ, 6^\circ, 13^\circ$ , for which the deviations of the FSR are compared with the FSR at  $\delta = 0^\circ$  and  $2\theta_0 = 0^\circ$  by subtracting that FSR as a base level. The FSR has been searched with the transmission spectrum for the wavelength range near 1520 nm, and the deviations of

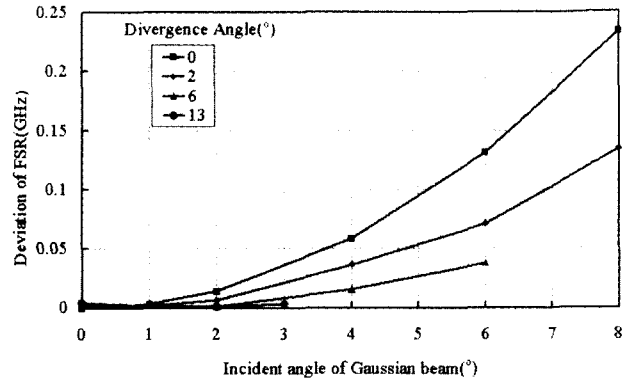


FIG. 4. Deviation of FSR as a function of incident angle and divergence angle compared with the FSR at  $\delta = 0^\circ$  and  $2\theta_0 = 0^\circ$ .

the FSR are obtained by difference from the FSR at  $\delta = 0^\circ$  and  $2\theta_0 = 0^\circ$  to the FSR for arbitrary angles. The simulated curve for  $2\theta_0 = 0^\circ$  is almost the same as the measured result for  $2\theta_0 = 0.25^\circ$ , for a nearly collimated beam, although it is not compared in the graph. As the result, the larger divergence angle of the laser beam for the etalon makes a smaller deviation of the FSR than for the slightly diverged beam, but it would be limited by the poor wavelength discrimination of the etalon at larger divergence angle as shown in Fig. 2 and Fig. 3, in spite of the benefit in relatively small deviation of the FSR. Otherwise, for a finely collimated laser beam, the larger incident angle for the etalon can make a larger deviation in the FSR, which creates a difficulty in the angle control for the exact period of the FSR.

With the angle effects, the temperature dependency of the FSR also is of interest, since the solid etalon with long cavity for a narrower FSR should be used with a temperature control system, such as a TEC or heater. Fig. 5 shows the calculated and measured temperature dependency for transmission spectrum from  $25^\circ\text{C}$  to  $55^\circ\text{C}$ . The deviation of the FSR and the

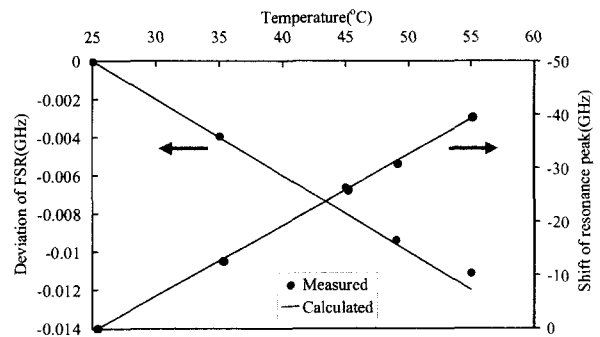


FIG. 5. Deviation of FSR and shift of resonance peak as a function of etalon temperature for  $25^\circ\text{C}$ . The divergence angle of Gaussian beam is  $2\theta_0 = 0.5^\circ$ .

shift of the transmission peak are calculated from (4), which can be easily expressed as a function of the FSR and the resonance order for transmission peaks. The temperature change of 30°C for the etalon makes about 40 GHz of frequency shift for the resonance peak in the transmission spectrum, and it generates about -0.012 GHz of deviation compared with the FSR at 25°C. Above all, the increased temperature induces a negative change in the FSR, while the increased incident angle induces a positive change of the FSR for a slightly diverged beam. The results confirm that the temperature tuning for the etalon is useful to minimize the deviation of the FSR as an optional way to compensate the undesirable errors generated in angle alignment of the etalon, and also to rearrange the periodic transmission spectrum for multi-channel ITU grid.

#### IV. CONCLUSION

The detail spectral characteristics of a solid etalon with 50 GHz spacing were investigated with variable incident angle for the diverged laser beam and with the temperature change of the etalon. With the theoretical and experimental analyses, the spectra for the incident angle of the diverged laser beam were well understood to predict the proper wavelength discrimination in a laser module packaged with an etalon and a normal size of PD. The results also confirmed that the FSR of the etalon could be adjusted by the direct temperature control for the etalon to compensate the misaligned incident angles. This is very useful for creating the full channel coverage for the wide-band DWDM application, as presented in [8].

\*Corresponding author : jd03@etri.re.kr

#### REFERENCES

- [1] T. Wipiejewski, Y. A. Akulova, G. A. Fish, P. C. Koh, C. Schow, P. Kozodoy, A. Dahl, M. Larson, M. Mack, T. Strand, C. Coldren, E. Hegblom, S. Penniman, T. Liljeberg, and L. A. Coldren, "Performance and reliability of widely tunable laser diodes," *Electronic Components and Technology Conf. Proc.*, pp. 789-795, May. 2003.
- [2] Jill D. Berger, Yongwei Zhang, John D. Grade, Howard Lee, Stephen Hrinaya, and Hal Jerman, "Widely tunable external cavity diode laser based on a MEMS electrostatic rotary actuator," *Optical Fiber Communications Conf. Proc.*, Tuj2-1-Tuj2-3, Mar. 2001.
- [3] B. Villeneuve, M.Cyr, and H.B.Kim, "High-stability wavelength-controlled DFB laser sources for dense WDM applications," *Optical Fiber Communications Conf. Proc.*, pp. 381-382, Feb. 1998.
- [4] H. Nasu, T. Mukaihara, T. Takagi, M. Oike, T. Nomura, and A. Kasukawa, "25-GHz-spacing wavelength-monitor integrated DFB laser module for DWDM applications," *IEEE Photon. Technol. Lett.*, vol. 15, pp. 293-295, Feb. 2003.
- [5] B.E.A. Saleh and M.C.Teich, "Beam optics" *Fundamentals of Photonics*, New York: John Wiley & Sons, pp. 81-91, 1991.
- [6] J. S. Browder, S. S. Ballard, and P. Klocek, "Physical properties of glass infrared optical materials," *Handbook of infrared optical materials*, vol. 30 of Optical Engineering, P.Klocek, Ed. New York: McGraw-Hill, pp. 445-448, 1991.
- [7] Jae-Seung Lee and Chang-Sup Shim, "Characteristics of a spectrum-slicing filter composed of an angle-tuned Fabry-Perot etalon and a Gaussian input beam," *IEEE Photon. Technol. Lett.*, vol. 7, pp. 905-907, Aug. 1995.
- [8] J.D. Kim, K.S. Choi, H.G. Yun, B.S. Choi, J.H. Lee, Y.S. Um, S.I. Kim, H.S. Go, and J.T. Moon, "Internal wavelength locker for ITU 50 GHz spacing", *Proc. Photonics Conference (Jeju, Korea)*, F2E3, pp. 741-742, Nov. 2003.